Response to Referee #1
Warm protons at comet 67P/Churyumov-Gerasimenko – Implications for the infant bow shock

We thank the referee for the comments and suggestions. We have made the necessary amendments to the paper and answers to comments may be found below. (Blue: Referee comment, black: our answer).

Line 65: More justification is needed as to why the warm proton flux is used as the main signal of the shock over other parameters, or over being used in conjunction with other parameters. The discussion mentions reasons as to why other parameters are not sufficient, i.e. hot electrons might be missed. Such arguments should be moved up in the manuscript and used as an assumption and justification for using the warm protons. What other phenomena could produce warm protons?
Line 245 states that some events could be examples of phenomena other than a weak shock. What are the comparative phenomena? Line 130 mentions some other effects such as changes in solar wind velocity/density/cometary ion density but these aren't adequately described or referenced. This discussion on alternate production mechanisms for warm protons is central to the arguments being made in this manuscript and ties back to my first point regarding Line 65.
We added the following after the sentence on lines 65-67 (line numbers referring to the previous version of the manuscript): "According to Balogh & Treumann (2013) , the slowing down and heating of the medium over a narrow layer or boundary is the defining feature of any shock." Near line 130 (again old numbering) we added a few words of explanation by changing "can also cause warm protons to appear" to "can also move the boundary, causing warm protons to appear at the spacecraft". We also added a reference.

Line 155: The selection criteria is outlined as a 'pronounced decrease' in the proton energy and a 'broadening of the energy band'. Figure 2a however shows values above and below unity, does this not contradict the selection criteria? If vm,h in Figure 2 is different to the H+ (E/q) column in Table 1 this needs to be described. Some clarity is needed here.
The solar wind energy spectra measured by Rosetta are difficult to condense into a reliable parameter that can be used for statistics. Further investigation has revealed that often the $v_{m,H}$ parameter is not a good representation of what is visible in the spectra, due to cross-talk, field of view and noise issues. In this updated version of the paper we therefore have omitted the statistical study of the $v_{m,H}$ parameter, as the results are not reliable.

Line 200: Statistics such as Figure 2 (can (a) be quantitatively represented on line 200 with a percentage?), 60% electron energy increase on line 205, 68% on line 210 for the B field decrease, 52% on line 210 for the s/c potential decrease, indicate to me that the detection criteria for the Infant Bow Shock is not sufficient – i.e. the shock has not been persistently detected.
For the statistics on the velocity, see answer above. As stated in Section 2.2, we do not use the magnetic field, or the s/c potential (now density) to identify an infant bow shock. We simply are looking at where these transitions from a cold, fast solar wind to a warm, slow solar wind occur. The statistics presented here are just a result, and not a criterion.

Line 40: There isn't mention of an induced magnetopause or the plasma boundaries referred to in the first line of the abstract. Surely this should follow on from the introduction to how an observable shock forms due to increased mass loading. Where is the induced magnetopause expected to form in relation to where these events are detected? Could these events be associated with this instead?
In our current understanding of the comet's interaction with the solar wind, no induced magnetopause exists. This concept is often used at Mars/Venus, but it is not used at the comet. The boundaries that are observed at the comet are a solar wind ion cavity (e.g. Nilsson et al. 2017 MNRAS), a diamagnetic cavity (e.g. Goetz et al 2016 A&A) and there are some indications of

a collisionopause, i.e. a tenuous boundary where collisional coupling of ions or electrons to the neutral gas become important (Mandt et al 2016 MNRAS). The diamagnetic cavity and the collisionopause lie within the solar wind ion cavity and the solar wind ion cavity by definition is the region that does not contain any solar wind ions. Thus, the boundary that we observe here lies outside of all of these boundaries and is distinct from them. We have added a paragraph in the introduction similar to this explanation.

Line 160: The use of the spacecraft potential is I believe not appropriate. That the spacecraft potential follows the density is only true when assuming a constant temperature. This study is focused on studying a shock which will alter and heat the plasma.

Johansson et al (2020) showed that the Rosetta spacecraft potential is predominantly dependent on density and only found a weak dependence on temperature of the electrons. It is thus a good indicator of density even when the temperature changes. Since the writing of this manuscript a more reliable density dataset has become available and thus, for this version of the manuscript, we changed from spacecraft potential to density. As expected, this does not change the results. The implications of these statistics are then discussed in the next paragraphs.

Line 240: This sentence is an evaluation of the hypothesis of whether these events are indeed the shock. 250 to 270 then appears to go into some, perhaps reasonable but certainly speculative, arguments about why the statistics are not good. The study therefore, with reference to line 345 and 355, seems to go on to imply that all warm proton detections are associated with the shock. This may be true but is not supported by the analysis presented. See point below: Line 345: The sentence "All parameters, except for the magnetic field magnitude, behave according to what was defined for the infant bow shock" doesn't seem to me to agree with the statistics presented in Figure 2 and the next sentence which states that only 10% agree. Some clarity is needed here.

The apparent contradiction comes from the statement about the 10 %. We have revised that sentence to clarify: "In about 10 % of the cases all parameters that were evaluated, the magnetic field included, behave as expected at the same time."

Line 355: The study concludes that the shock is an asymmetric structure persistently observed. This to me is in contradiction to the statistical results - surely the conclusions are that the shock is not persistently detected given many of the statistics are not much better than tossing a coin. It is this aspect of the paper that I feel is biased in a certain direction and therefore draws conclusions not fully supported by the data.

As discussed in the text for $v_{m,H}$, this parameter is not very well suited for usage in a statistical study. It needs to be treated with caution, which we have done for the smaller subset of events, but chose not to do for the large dataset. A reexamination of the parameter has reaffirmed this. To avoid confusion, this parameter was removed from figure 3 and is only discussed in the text now. The defining features of a shock, which we have used to select the events, are the heating and slowing down of the streaming plasma. This applies for all the observed cases for the ion spectra. The other quantities, shown in Fig. 2, should be seen as descriptive rather than defining, and as such do not invalidate the conclusions. This was also made clearer already in the abstract.

Line 220: Heliocentric distance I think should be mentioned before now to orient the reader. How are the 370 events selected? How many Rosetta orbits are there in total outside the cavity? How many with good data that the 370 are selected from? Some explanation and context is needed here for reproducibility. I recommend changing Line 110 to include this information.

As Rosetta is near an object with very low gravity, most of the time there is no bound orbit. In principle, Rosetta is orbiting the Sun along side the comet. The trajectory is highly complex and cannot be quantified simply as orbits within a certain region. We have used the entire dataset, as stated in Section 2.2, to find these events. Figure 3 shows the cometocentric distance for the entire mission in grey, thus we do provide information on the spacecraft-comet separation.

Figure 4 (left panel) shows the coverage of Rosetta in the CSE frame. The PSA was referenced and a link to the spice kernels is provided in the referenced Rosetta PSA website. It is therefore possible to reproduce everything shown here, including the event locations, as given in the supplementary material.

Line 40: Can the "few percent" be better constrained or referenced with respect to 67P?

For the event from Figure 1 we can derive a proton density of ca $0.5\,\mathrm{cm}^{-3}$ from the ICA moments. The plasma density is of the order of $1000\,\mathrm{cm}^{-3}$, this would mean a proton fraction of 0.05%. This seems rather low, however, the proton density estimate is also extremely low. Even assuming that ICA underestimate by a factor of 10, would only give us a fraction of 0.5%. Thus, for the larger plasma dynamics, the protons can be neglected. Alternatively we can make an estimate of the maximum proton density based on a simple fluid model, which seems a better way to get the maximum fraction of protons in the plasma. We have added to the paper: " We can estimate the fraction of cometary ions for the event shown in Fig. 1. The cometary ion density is of the order of $1000\,\mathrm{cm}^{-3}$ and we can estimate the maximum proton density from a simple back-of-the-envelope calculation: assuming a solar wind density of $3\,\mathrm{cm}^{-3}$ (typical for heliocentric distances around 2 AU) and a compression factor of ~ 4, we get a proton density of $12\,\mathrm{cm}^{-3}$. This is close to what is also observed in the simulation used below. This gives a fraction of $\sim$ 99% cometary ions. Even if this estimate is very rough, it is clear that the cometary ions are at this point clearly dominating the plasma and the solar wind has only very little influence on the plasma density."

Line 70: Should "easily" be "earlier" instead?

Indeed, this was corrected.

Line 100: Can you please reference the "is believed".

Yes, explanations can be found in Johansson et al 2020, which was added to the text.

Line 130: What publications does the "(as stated in previous publications)" refer to?

This refers to Gunell et al 2018 and is now explicitly mentioned in the text.

Line 159: Why is the following sentence interesting? "Interestingly, the flux diminishes at the same time that the proton energy increases gradually."

We have clarified the statement: "Interestingly, the flux diminishes at the same time that the proton energy increases gradually, implying that the spacecraft moved slowly upstream in a shock-fixed frame of reference into a region with less electron heating and a less slowed-down proton distribution."

Line 265: The description of the solar wind "pushing" the shock is not accurate, shocks are modes as opposed to pressure balanced structures. Rewording is needed.

This is indeed correct. We reworded the sentence: "One possibility is that an increase in the solar wind dynamic pressure increases the mass-loading threshold of the plasma (Biermann et al 1967) which means that the critical condition for a shock is met later in the flow, and thus closer to the comet. "

Line 308: I do not believe the authors have "made attempts to conclusively show that this structure is indeed a shock in the fluid dynamics sense." This is far too strong and I think would only be correct if sufficient effort had been made to deal with the RH jump conditions.

In a first attempt, we indeed tried to evaluate the R-H conditions for one event. However, as detailed in the text, this is a moot point because the R-H conditions are not applicable here. But, in order to avoid any misunderstandings, this sentence was changed to a more generic: "In order to provide proof that a boundary in a plasma is a shock, usually Rankine-Hugoniot are evaluated."

Significant Text Changes

~~Multiple plasma boundaries have been observed at~~ The plasma around comet 67P/Churyumov-Gerasimenko ~~. Among them was an~~ shows remarkable variability throughout the entire Rosetta mission. Plasma boundaries such as the diamagnetic cavity, solar wind ion cavity and infant bow shock ~~, an asymmetric structure~~ separate regions with distinct plasma parameters from each other. Here, we focus on a particular feature in the plasma~~environment that separates the less disturbed solar wind from a plasma with warmer, slower protons. Rosetta crossings of the infant bow shock have so far only been reported for two days. Here, we aim to investigate this phenomenon~~ : warm, slow solar wind protons. We investigate this particular proton population further by focusing on the proton behaviour and surveying all of the Rosetta comet phase data. We find over 300 events ~~that match the proton signatures at the infant bow shock~~where Rosetta transitted from a region with fast, cold protons into a region with warm, slow protons.

~~Both~~ These results agree well with simulations of the infant bow shock (IBS), an asymmetric structure in the plasma environment previously detected on only two days during the comet phase. The properties of the plasma on both sides of this structure

As a comet approaches the Sun, energy input into the surface increases ~~and with it~~ which increases the amount of ice that is sublimated and escapes into space.

At higher gas production rates this asymmetry is less pronounced and the influence of the cometary ion gyroradius is diminished, because the magnetic field pile-up at the comet results in higher field magnitudes and thus ~~lower gyroradii.~~ smaller gyroradii.

Boundaries in the plasma at 67P have been identified and characterized in many publications. The three main boundaries that were observable by Rosetta were, in order of decreasing cometocentric distance, the solar wind ion cavity (e.g. Nilsson et al., 2017), a collisionopause (Mandt et al., 2016), and the diamagnetic cavity (e.g. Goetz et al., 2016a,b). The solar wind ion cavity is the region where no solar wind ions can be observed in the plasma, from May 2015 to January 2016 Rosetta was almost exclusively within this region. The collisionopause demarcates the tenuous boundary where ion-neutral or electron-neutral collisions become important and it has been shown to lie within the solar wind ion cavity. Finally the diamagnetic cavity is the innermost observed region, where the magnetic field is very close to zero. For a more detailed overview of these boundaries see e.g. Götz et al. (2019).

Another boundary in the plasma environment of a comet, but not observed by Rosetta, is the bow shock.

There, the interaction between the solar wind and the comet cannot be described by mass-loading alone, instead the flow changes from supersonic to subsonic and a bow shock forms. This prediction is shown to fit well with observations at e. g. comet Halley (Neubauer et al., 1986), where the bow shock was detected 1.15×10^6 km from the nucleus. The transition from unshocked to shocked solar wind was identified by a decrease in speed, increase in density and temperature and an increase in the magnetic field (Coates et al., 1990). The shock was identified as a low Mach number shock, in agreement with the model, which predicted a gradual slowing of the solar wind flow already upstream of the shock due to the incorporation of the cometary ions. The cometary ion density is often neglected in bow shock models at high activity comets, because it only reaches 1.5-2.5% of the total density. Observations of bow shocks at other comets where quite similar, although at the lower activity comets Giacobini-Zinner (GZ) and Grigg-Skjellerup (GS) the bow shock is often termed a bow wave, due to the lack of a sharp boundary (Smith et al., 1986). At GS, a strong non-gyrotropy of the cometary ions could be observed near the bow wave, together with wave activity triggered by this unstable distribution function (Coates et al., 1996). Koenders et al. (2013) compare the bow shock distances from a simple single-fluid model with distances gained from Hybrid simulations and find that the fluid models predicted consistently higher stand off distances. Thus, the ion gyroradius effects are pronounced even in the most fluid-like stage of the plasma around comet 67P. ~~The shock~~

The shock itself forms by waves steepening into the nonlinear regime. The speed of the steepened wave is faster than that of the linear wave, but steepening is counteracted by dissipation. If an obstacle and a plasma are in relative motion faster than the speed of linear waves, the waves steepen until an equilibrium is reached where the shock becomes a stationary wave in the obstacle~~, in this case~~ 's (the comet's~~,~~) frame of reference (Balogh and Treumann, 2013).

~~Koenders et al. (2013) compare the bow shock distances from a simple single-fluid model with distances gained from Hybrid simulations and find that the fluid models predicted consistently higher stand off distances. Thus, the ion gyroradius effects are pronounced even in the most fluid-like stage of the plasma around comet 67P.~~

DIFaddbegin According to Balogh and Treumann (2013) , the slowing down and heating of the medium over a narrow layer or boundary is the defining feature of any shock.

Often, the signal is then still visible in the RPC-IES instrument, as the FOV is partially complimentary (rotated by 60°), a detailed description of the FoV can be found in the ICA User Guide on the PSA[1]. Solar wind

[1] https://cosmos.esa.int/web/psa/rosetta

Start time	H^+ E/q	$\Gamma_{IES,e}$	B_m	P_B	cos(θ)	~~$V_{s/c}$~~ n_{pl}	T_p	H^+ E/q	$\Gamma_{IES,e}$	B_m	P_B	cos(θ)	~~$V_{s/c}$~~
Dec 07, 14 03:49	↓	↑	–	↓	–	–	↑	↑	–	–	–	–	
Dec 25, 14 09:50	↓	↑	↓	↓	–		↑	↑	↓	–	–	–	
Jan 04, 15 12:19	↓	↑	–	↓	–		↑	↑	–	–	↑	–	
Jan 04, 15 19:55	↓	↑	↑	–	–		–	↑	↓	↑	–	↓	
Mar 07, 15 05:48	↓	↑	↑	↑	↑		↓	↑	↓	↓	–	↓	
Feb 10, 16 09:02								↑	↓	↓	↓	↓	
Feb 26, 16 05:50	↓	–	–	–	–	–	–	↑	–	↓	–	↓	
Feb 29, 16 00:27	↓	–	–	–	↓	–	–	↑	↓	↓	↓	↑	
Apr 08, 16 03:27	↓	↑	↓	↓	↑	↑		↑	↓	↑	↑	↓	
Apr 08, 16 07:58	↓	↑	↓	↑	–	↑	–	↑	↓	↑	–	↓	
Jun 01, 16 12:11	↓	↑	↑	↑	↑	–↑	↑						
Jul 09, 16 12:43	↓	↑	↑	↑	–	↑	↑	↑	↓	–	–	↓	
Jul 09, 16 15:52	↓	↑	↓	↓	–	↑	↑	↑	↓	–	–	↑	
Median	↓	↑	–	–	–	–↑	↑	↑	↓	–	–	↓	

Table 1: List of 13 events chosen for a more detailed study and list of parameter changes when crossing from upstream to downstream (inward, left) and from downstream to upstream (outward, right). The last line summarizes events by giving a median change. Missing signs indicate that no data was available.

densities near the comet also decrease due to significant charge exchange losses (Simon Wedlund et al., 2019). This caused rather low densities in the times when Rosetta was just outside the solar wind ion cavity. The RPC-ICA ~~moments~~ solar wind moments, including the temperature, used in this study are integrations of the RPC-ICA PSA L4 PHYS-MASS data set, also delivered to the planetary science archive (PSA) as RPC-ICA L5 MOMENT data set. ~~We chose to use the mean proton speed $v_{m,H}$ derived from this data set for assessment of the speed near the IBS. This value is derived by calculating the mean velocity of the proton energy distribution and thus is a more suitable parameter than the 3D velocity moment which is heavily influenced by the pitch angle distribution of the protons (Behar et al., 2017). Here, we only use values for which the density of the protons (calculated from the flux) is above 0.005 cm^{-3} which is the case for about 90% of all values.~~

~~Its FoV is partially complementary to ICA, but the~~ The time resolution is at least 256 s~~. The~~ , and the measurements at low energies are disturbed by the spacecraft potential, which is between 0 V and −20 V most of the time.

~~.~~ (Johansson et al., 2020). For this study, we use the density estimate to characterize the plasma.

~~These are the two criteria used~~ For the first criterion, the threshold was a shift of the peak of the ion spectra by at least three energy bins, corresponding to at least 60 eV. We only use these two criteria for detection. For verification we evaluate additional properties like the ICA derived proton temperature, plasma density, suprathermal electron fluxes, magnetic field magnitude power spectral density in the frequency range between 50 mHz and 75 mHz and the magnetic field magnitude. However, the direction of change (increase or decrease) is not considered, ~~instead~~ because the change in parameters is simply an indicator that the change in proton energy and flux is not due to instrumental or spacecraft effects.

We also use the sun aspect angles of the spacecraft to exclude an attitude change of the spacecraft as a reason for a change in the proton signal. These are defined as the angles of the three spacecraft axes to the Sun-comet line[2]. Events that coincide with major attitude changes (> 10°) are not included in the study.

Other parameter changes like solar wind velocity and density as well as cometary ion density can also ~~cause~~ move the boundary, causing warm protons to appear ~~(as stated in previous publications)~~ at the spacecraft (as stated in Gunell et al., 2018).

The He^+ and He^{2+} show a very similar behaviour to the protons (panel a), decreasing and broadening in energy, but their signature remains distinct from each other at all times. The IES electron signature (panel d) increases in energy and flux. Interestingly, the flux diminishes at the same time that the proton energy increases gradually~~.~~ , implying that the spacecraft moved slowly upstream in a shock-fixed frame of reference into a region with less electron heating and a less slowed-down proton distribution. This is similar to what was observed already by Gunell et al. (2018).

This is because θ represents the angle between the x-axis and ~~magnetic~~ electric field, thus it does not reflect changes in the z-component of the magnetic field very well. The ~~spacecraft potential~~ plasma density (panel h) ~~is lower in the downstream region. We use this as a proxy for the density of the plasma: the lower the spacecraft potential, the higher the density. Thus the density is higher in the downstream region. We also ensure that these changes in the particle signatures are not due to a change in FoV, thus we included the spacecraft attitude~~ as well as the proton temperature (panel i) ~~to confirm that it only changes insignificantly in the time interval~~

[2] See https://www.cosmos.esa.int/web/spice/spice-for-rosetta

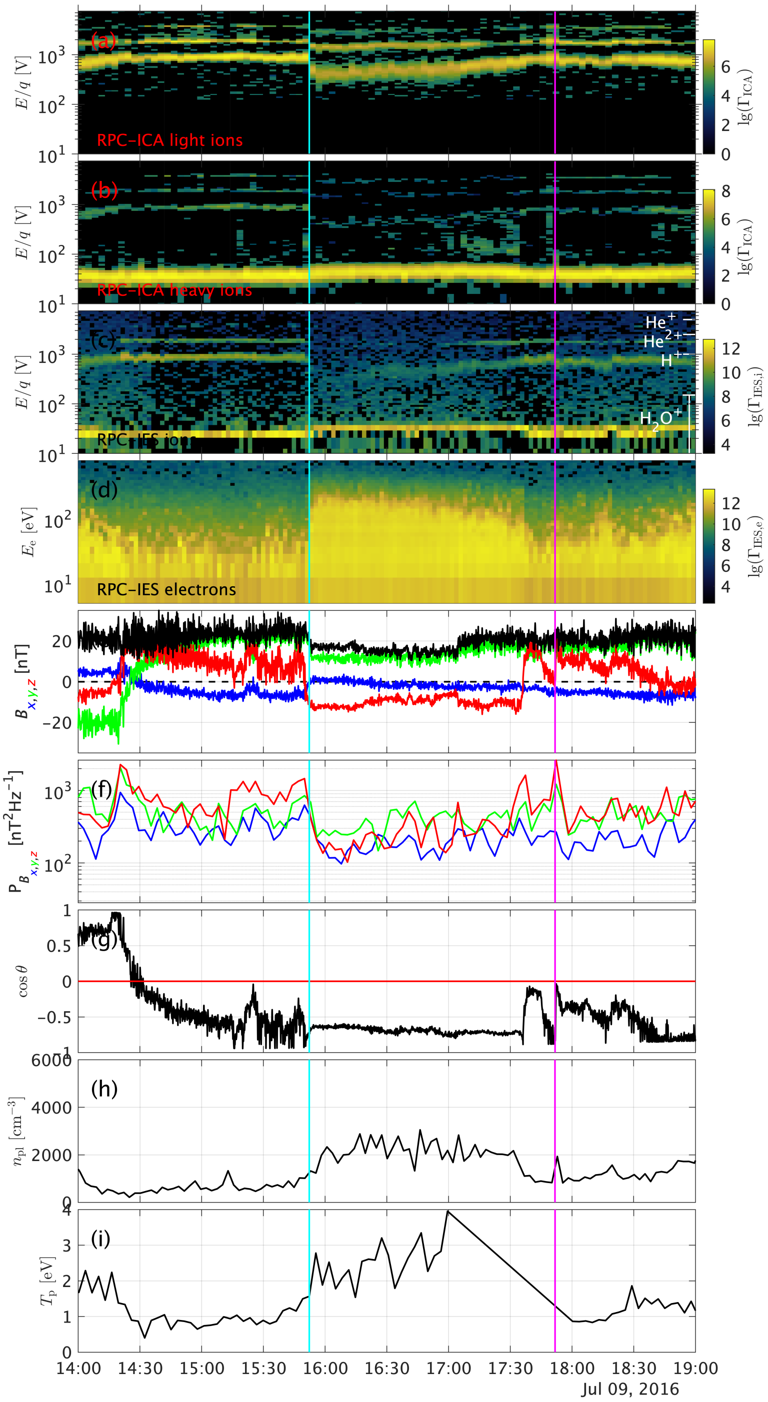

Figure 1: Observations of the event on July 9th, 2016. From top to bottom: a) ICA solar wind ions, b) ICA heavy ions, c) IES ions, d) IES electrons, e) magnetic field in CSEQ coordinates, f) magnetic power spectral density in the frequency range between 2 mHz and 15 mHz, g) angle between spacecraft position and convective electric field, h) ~~spacecraft potential~~plasma density from LAP, and i) ~~attitude~~1D proton temperature from ICA.

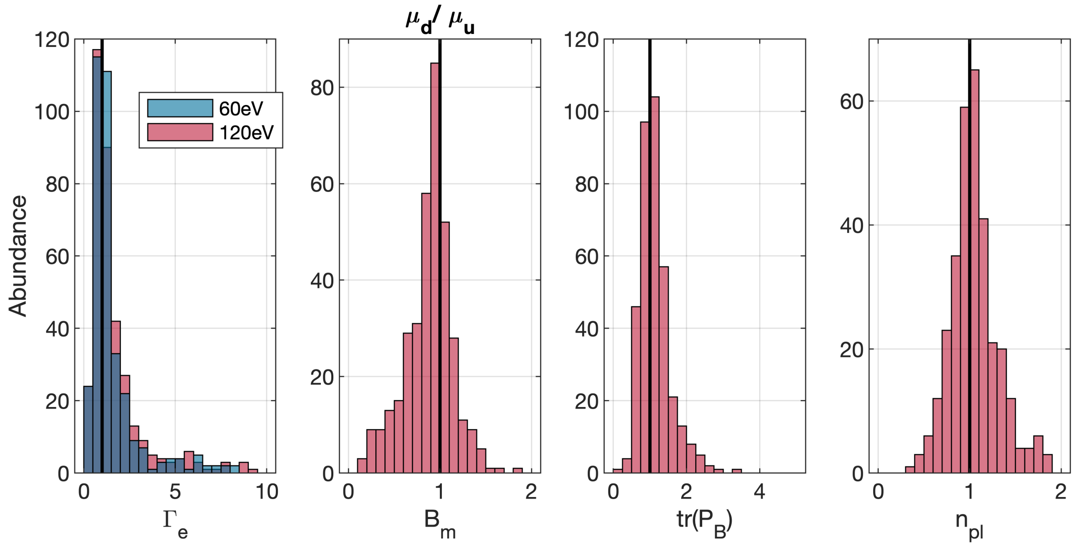

Figure 2: Comparison of the upstream and downstream mean values for five four of the six seven parameters chosen for investigation. From left to right: Electron flux Γ_e at 60 eV (blue) and at 120 eV (red), magnetic field strength B_m, trace of the magnetic field power spectral density tr(P_B), and plasma density n_{pl}.

in questionare higher in the downstream region.

The parameters that we use to characterize how the plasma changes at the boundary are the proton energy H^+ E/q, the flux of the electrons $\Gamma_{IES,e}$, the magnetic field magnitude B_m, the power spectral density of the magnetic field P_B, the angle cos(θ), and the spacecraft potential $V_{s/c}$the plasma density n_{pl}, and the proton temperature T_p. The changes are indicated in Table 1. Here, we are only looking at the qualitative changes, quantitative changes will be assessed in the next section, where the larger statistics should make up for the large uncertainty for each event. These clear, qualitative events can then be used to verify the quantitative, statistical outcome.

From these events we can conclude: Since the proton energy was used as a selection criterion the proton energy in the downstream region is always lower than upstream. The proton temperature is almost always higher in the downstream region. For the other parameters, we find that the energy of the electrons is almost always increased and the spacecraft potential is often lower density is often higher in the downstream region.

The statistical assessment of the proton flux is complicated by an incomplete FoV and the broad distribution of the protons. Therefore, moments of the distribution function are less representative in the situation at comet 67P. Instead, we use the mean speed of the protons: a simple 1D approximation of the energy spectra of the protons. This parameter does not represent the angular spread of the particles, but it is the most representative of the energy vs. time spectrograms that we used to identify events. Even this parameter is not always reliable, as it only uses ICA spectra and some events that were identified earlier are only (better) visible in the IES spectra. Therefore a direct statistical study of the moments cannot be conducted. To assess the electron flux changes, we chose two energy values (60 eV and 120 eV) to extract a 1D time series of the flux at these energies. They were chosen based on an inspection of the subset of events, were where these energy bands showed the clearest change.

These larger statistics agree mostly with the observations from the 13 events that were categorized by hand. From left to right:

$v_{m,H}$ The proton energy (decrease) and width of the energy spectra (increase) were originally chosen as selection criteria. The downstream to upstream ratio shows a larger number of values below than above unity as expected for a decrease in energy as was seen in Sect. ??. However, the mean speed of the protons does not always decrease. This is probably due to the way that the mean speed is calculated, as it is the centre of weight of the energy spectra. For a low signal-to-noise ratio, this value is not meaningful.

Γ_e In our smaller subset, the energy of the electrons in the 60 eV and 120 eV band increases in 10 of the 12 inbound passes and decreases in 8 of the 12 outbound passes. In the entire dataset the electron energy is increased in the downstream region in 60% of all cases. That the larger statistics do not show the same behaviour may in part be because the energy dependent electron flux is difficult to condense to a single parameter, and the instrument sensitivity declined significantly after perihelion. We have observed cases , where the flux was very low and thus changes were not visible.

B_m The magnetic field decreases in 68% of cases. This is consistent with the case studies above.

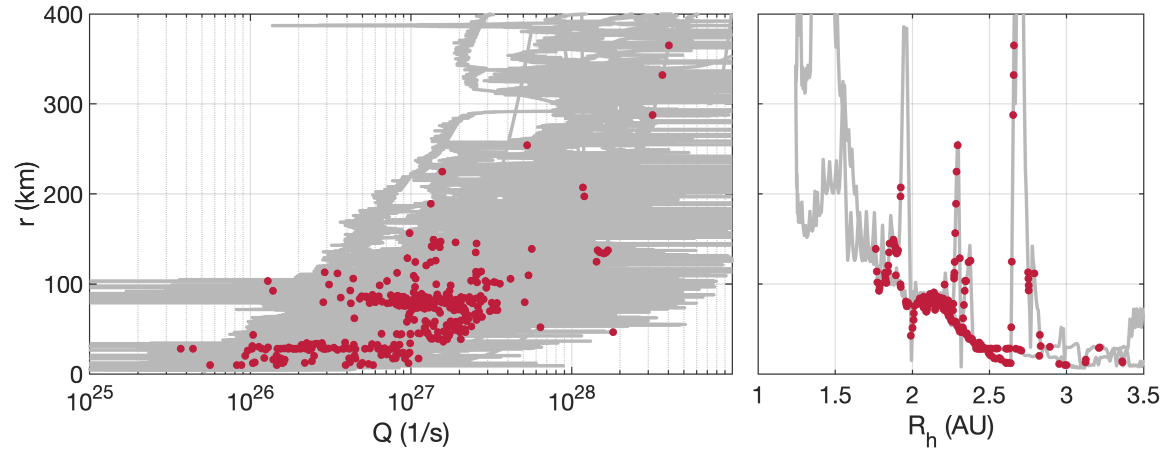

Figure 3: Cometocentric distance of the spacecraft over gas production rate (left) and heliocentric distance (right). The gas production rate was derived from measured neutral gas densities using a spherically symmetric model. The grey lines show the position during the entire Rosetta mission, while the red dots indicate boundary crossings.

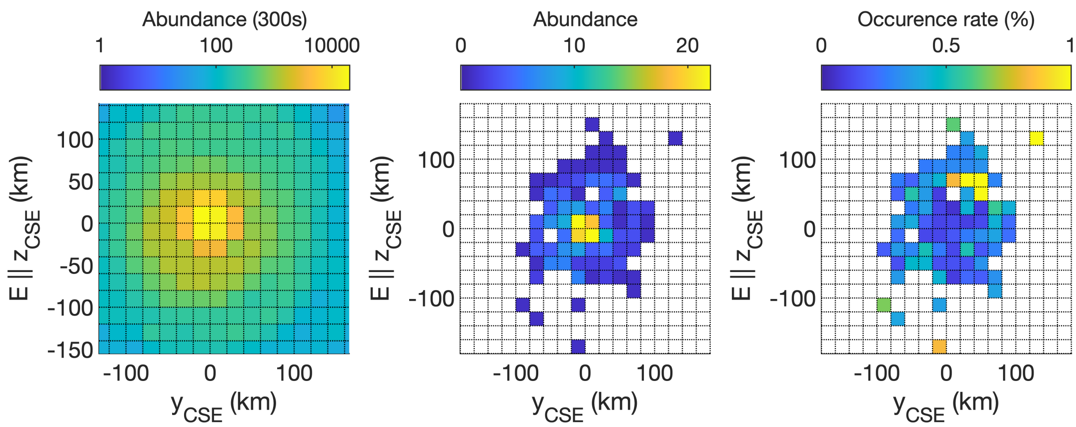

Figure 4: Abundance of the position of the spacecraft (left), position at which warm protons were detected (middle) and occurrence rate of detections normalized to the spacecraft dwell time (right). The $+E_c$ hemisphere is that of $z_{CSE} > 0$.

$\mathrm{tr}(P_B)$ The trace power spectral density increases downstream in 58% of all cases.

~~U_{sc} The spacecraft potential decreases~~

n_{pl} The plasma density increases in 52% of all cases. This is consistent with the case studies, where the ~~spacecraft potential was either decreased~~ density was either increased downstream or not changed at all.

The relevant gyroperiods of 0.5 s (protons) and 9 s (water ions) are much smaller than any of the transition times we observe. The behaviour of the magnetic field magnitude is an example of this. In shock modelling, the magnetic field is generally stronger on the downstream than the upstream side of the shock. In our statistics, we have many cases of the opposite behaviour. One possibility is that an increase in the solar wind dynamic pressure ~~pushes the~~ increases the mass-loading threshold of the plasma (Biermann et al., 1967) which means that the critical condition for a shock is met later in the flow, and thus closer to the comet. This moves the IBS further towards the ~~comet~~ nucleus and Rosetta passes into the upstream region, but at the same time the magnitude of the interplanetary field increases, resulting in a new, stronger magnetic field.

DIFdelbegin ~~When considering~~ We can also consider just the subset of events where the plasma behaves as expected for an IBS (the magnetic field increases downstream along with an increase in the power spectral density, increase in electron flux). ~~About 10% of all events fulfil all these criteria and one~~ In about 10 % of the cases all parameters that were evaluated, the magnetic field included, behave as expected at the same time. One such event is shown in Fig. ??. Although the ICA data is missing for the first half of the event (before 06:30), we can clearly see warm proton fluxes in the IES data ~~for the first half of the event. For the second half~~

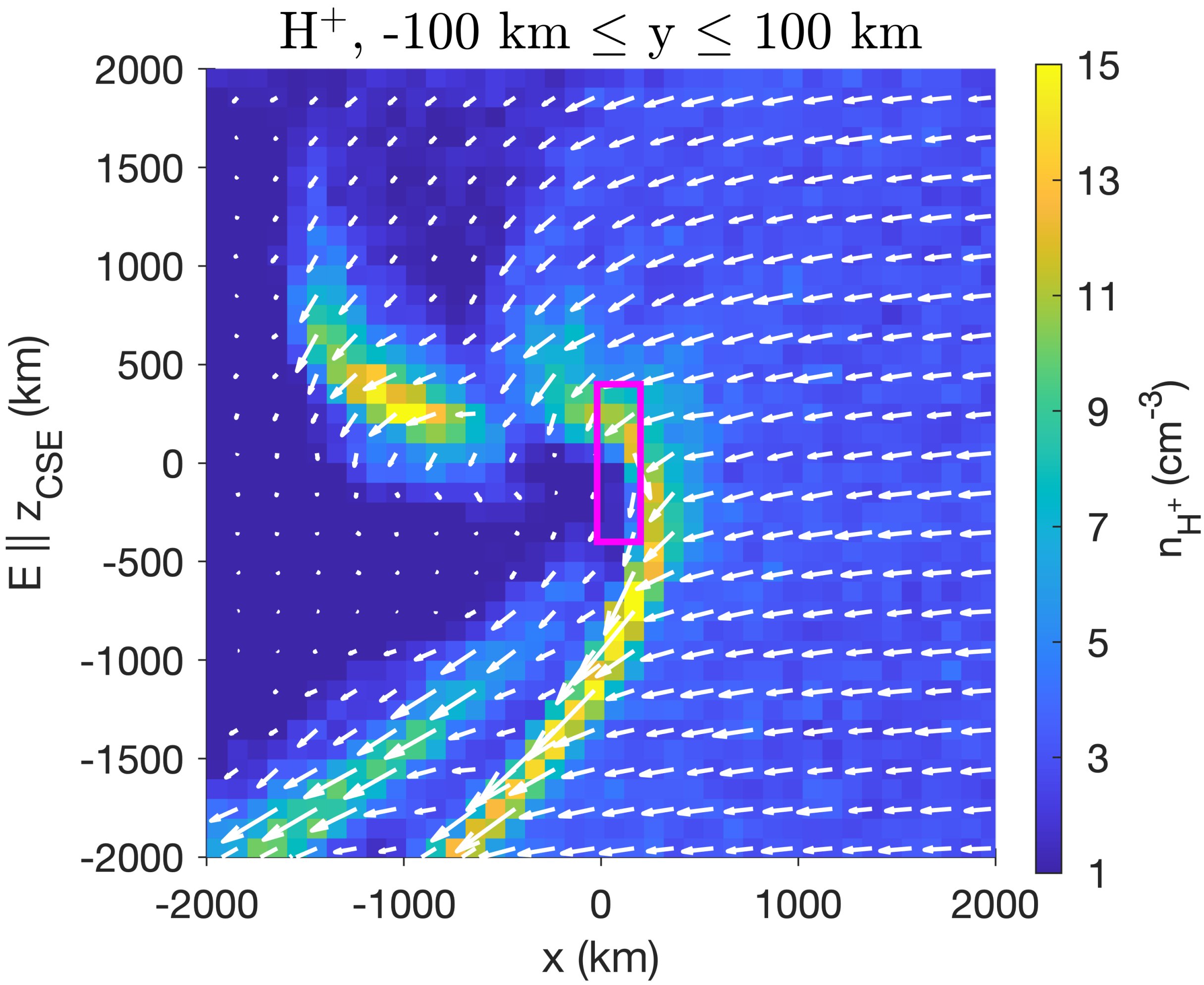

Figure 5: Density and direction of the flux of the protons from the Hybrid simulations. The simulation was run for a case of $Q = 3.2 \times 10^{27}\,\mathrm{s}^{-1}$. For a more detailed list of parameters see Gunell et al. (2018). Here, the Sun is to the right. The IBS is roughly located where the proton density reaches its highest values (yellow).

~~they are registered by ICA~~ while ICA is off. Once ICA is running, the protons do appear in the ICA energy spectra.

We present here also for the first time the ~~spacecraft potential~~ plasma density measurements for this boundary. We find that the ~~spacecraft potential, and by extension the~~ density of the plasma on average does not change significantly at the boundary. In fact, events where the plasma density increases, decreases and is unchanged can all be found in the data set. This was expected, as the plasma density at 67P at this point is dominated by the heavy ions and not the solar wind. ~~Thus, the~~ We can estimate the fraction of cometary ions for the event shown in Fig. 1. The cometary ion density is of the order of $1000\,\mathrm{cm^{-3}}$ and we can estimate the maximum proton density from a simple back-of-the-envelope calculation: assuming a solar wind density of $3\,\mathrm{cm^{-3}}$ (typical for heliocentric distances around 2 AU) and a compression factor of ~ 4, we get a proton density of $12\,\mathrm{cm^{-3}}$. This is close to what is also observed in the simulation used below. This gives a fraction of $\sim 99\%$ cometary ions. Even if this estimate is very rough, it is clear that the cometary ions are at this point clearly dominating the plasma density and the solar wind has only very little influence ~~on the plasma density~~density-wise. Instead **?** found that the solar wind and cometary ion momentum are of similar importance at the intermediate stage of cometary activity.

The gyroradii of protons in the $200 - 400\,\mathrm{km\,s^{-1}}$ range are $100 - 200\,\mathrm{km}$ in a $20\,\mathrm{nT}$ magnetic field. This is comparable to the thickness of the infant bow shock. The typical length scale of the structure in the upper left corner of Fig. 5 is about $10^3\,\mathrm{km}$, corresponding to approximately 2 gyroradii in the weaker magnetic field ($\sim 10\,\mathrm{nT}$) in that region.

~~We have made attempts to conclusively show that this structure is indeed a shockin the fluid dynamics sense~~In order to provide proof that a boundary in a plasma is a shock, usually Rankine-Hugoniot are evaluated. However, the plasma environment of the comet is far from a single fluid MHD plasma where the ~~Rankine-Hugoniot~~ R-H conditions could be used to investigate the transition. Such an approach has been employed in the past in the analysis of the Giotto flybys of comets 1P/Halley and 26P/Grigg–Skjellerup (Coates et al., 1990, 1997) . Kessel et al. (1994) expanded the fluid theory to include effects of multiple ion species. For our situation, multi-ion and kinetic scale effects~~need to~~, and the non-stationarity of the shock need be accounted for.

Omidi and Winske (1987) conducted one-dimensional hybrid simulations with the aim of modelling the spacecraft encounters with comets 1P/Halley and 21P/Giacobini-Zinner. They found that for oblique interaction (cone angle 55°), shocklets form in a region of large amplitude wave activity. These shocklets convect downstream, where they break up due to dispersion, and new ones form further upstream. Thus, the process is repeated in a way that resembles shock reformation at planets (e.g. Balogh and Treumann, 2013). Although it is possible that shocklets form and shock reformation occurs also at comet 67P under certain conditions, it is not the cause of the observations reported here. The shock encounters shown in Figs. 1, **??**, 6, and 7 do not display the repetitive transitions in a wave-dominated region that would be expected for the shocklets reported by Omidi and Winske (1987).

It ~~is~~ may be that the infant bow shock ~~that develops into the ordinary~~ is the low gas production rate manifestation of what becomes the more developed cometary bow shock as ~~the comet moves closer to the Sun and the outgassing increases further~~observed at larger comets such as Halley.

References

André Balogh and Rudolf A. Treumann. *Physics of Collisionless Shocks*, volume 12 of *ISSI Scientific Report Series*. Springer, New York, NY, 2013. ISBN 978-1-4614-6099-2. doi: 10.1007/978-1-4614-6099-2.

E. Behar, H. Nilsson, M. Alho, C. Goetz, and B. Tsurutani. The birth and growth of a solar wind cavity around a comet - Rosetta observations. *MNRAS*, 469:S396–S403, July 2017. doi: 10.1093/mnras/stx1871.

L. Biermann, B. Brosowski, and H. U. Schmidt. The interactions of the solar wind with a comet. *Solar Physics*, 1:254–284, March 1967. doi: 10.1007/BF00150860.

A. J. Coates, A. D. Johnstone, R. L. Kessel, D. E. Huddleston, and B. Wilken. Plasma parameters near the comet Halley bow shock. *J. Geophys. Res.*, 95:20701–20716, December 1990. doi: 10.1029/JA095iA12p20701.

A. J. Coates, A. D. Johnstone, and F. M. Neubauer. Cometary ion pressure anisotropies at comets Halley and Grigg-Skjellerup. *J. Geophys. Res.*, 101(A12):27573–27584, December 1996. doi: 10.1029/96JA02524.

A. J. Coates, C. Mazelle, and F. M. Neubauer. Bow shock analysis at comets Halley and Grigg-Skjellerup. *J. Geophys. Res.*, 102(A4):7105–7113, April 1997. doi: 10.1029/96JA04002.

C. Goetz, C. Koenders, K. C. Hansen, J. Burch, C. Carr, A. Eriksson, D. Frühauff, C. Güttler, P. Henri, H. Nilsson, I. Richter, M. Rubin, H. Sierks, B. Tsurutani, M. Volwerk, and K. H. Glassmeier. Structure and evolution of the diamagnetic cavity at comet 67P/Churyumov-Gerasimenko. *MNRAS*, 462:S459–S467, November 2016a. doi: 10.1093/mnras/stw3148.

C. Goetz, C. Koenders, I. Richter, K. Altwegg, J. Burch, C. Carr, E. Cupido, A. Eriksson, C. Güttler, P. Henri, P. Mokashi, Z. Nemeth, H. Nilsson, M. Rubin, H. Sierks, B. Tsurutani, C. Vallat, M. Volwerk, and K.-H. Glassmeier. First detection of a diamagnetic cavity at comet 67P/Churyumov-Gerasimenko. *A&A*, 588:A24, April 2016b. doi: 10.1051/0004-6361/201527728.

Charlotte Götz, Herber Gunell, Martin Volwerk, Arnaud Beth, Anders Eriksson, Marina Galand, Pierre Henri, Hans Nilsson, Cyril Simon Wedlund, Markku Alho, Laila Andersson, Nicolas Andre, Johan De Keyser, Jan Deca, Yasong Ge, Karl-Heinz Glaßmeier, Rajkumar Hajra, Tomas Karlsson, Satoshi Kasahara, Ivana Kolmasova, Kristie LLera, Hadi Madanian, Ingrid Mann, Christian Mazelle, Elias Odelstad, Ferdinand Plaschke, Martin Rubin, Beatriz Sanchez-Cano, Colin Snodgrass, and Erik Vigren. Cometary Plasma Science – A White Paper in response to the Voyage 2050 Call by the European Space Agency. *arXiv e-prints*, art. arXiv:1908.00377, Aug 2019.

Herbert Gunell, Charlotte Goetz, Cyril Simon Wedlund, Jesper Lindkvist, Maria Hamrin, Hans Nilsson, Kristie Llera, Anders Eriksson, and Mats Holmström. The infant bow shock: a new frontier at a weak activity comet. *A&A*, 619:L2, November 2018. doi: 10.1051/0004-6361/201834225.

F. L. Johansson, A. I. Eriksson, N. Gilet, P. Henri, G. Wattieaux, M. G. G. T. Taylor, C. Imhof, and F. Cipriani. A charging model for the Rosetta spacecraft. *A&A*, 642:A43, October 2020. doi: 10.1051/0004-6361/202038592.

R. L. Kessel, A. J. Coates, U. Motschmann, and F. M. Neubauer. Shock normal determination for multiple-ion shocks. *J. Geophys. Res.*, 99(A10):19359–19374, October 1994. doi: 10.1029/94JA01234.

C. Koenders, K.-H. Glassmeier, I. Richter, U. Motschmann, and M. Rubin. Revisiting cometary bow shock positions. *Planetary and Space Science*, 87:85–95, October 2013. doi: 10.1016/j.pss.2013.08.009.

K. E. Mandt, A. Eriksson, N. J. T. Edberg, C. Koenders, T. Broiles, S. A. Fuselier, P. Henri, Z. Nemeth, M. Alho, N. Biver, A. Beth, J. Burch, C. Carr, K. Chae, A. J. Coates, E. Cupido, M. Galand, K.-H. Glassmeier, C. Goetz, R. Goldstein, K. C. Hansen, J. Haiducek, E. Kallio, J.-P. Lebreton, A. Luspay-Kuti, P. Mokashi, H. Nilsson, A. Opitz, I. Richter, M. Samara, K. Szego, C.-Y. Tzou, M. Volwerk, C. Simon Wedlund, and G. Stenberg Wieser. RPC observation of the development and evolution of plasma interaction boundaries at 67P/Churyumov-Gerasimenko. *MNRAS*, 462:S9–S22, November 2016. doi: 10.1093/mnras/stw1736.

F. M. Neubauer, K. H. Glassmeier, M. Pohl, J. Raeder, M. H. Acuña, L. F. Burlaga, N. F. Ness, G. Musmann, F. Mariani, M. K. Wallis, E. Ungstrup, and H. U. Schmidt. First results from the Giotto magnetometer experiment at comet Halley. *Nature*, 321:352–355, May 1986. doi: 10.1038/321352a0.

H. Nilsson, G. Stenberg Wieser, E. Behar, H. Gunell, M. Galand, C. Simon Wedlund, M. Alho, C. Goetz, M. Yamauchi, P. Henri, and E. Odelstad A.I. Eriksson. Evolution of the ion environment of comet 67P during the rosetta mission as seen by RPC-ICA. *Monthly Notices of the Royal Astronomical Society*, 469 (Suppl_2):S252–S261, 2017. doi: 10.1093/mnras/stx1491.

N. Omidi and D. Winske. A kinetic study of solar wind mass loading and cometary bow shocks. *J. Geophys. Res.*, 92(A12):13409–13426, December 1987. doi: 10.1029/JA092iA12p13409.

C. Simon Wedlund, E. Behar, H. Nilsson, M. Alho, E. Kallio, H. Gunell, D. Bodewits, K. Heritier, M. Galand, A. Beth, M. Rubin, K. Altwegg, M. Volwerk, G. Gronoff, and R. Hoekstra. Solar wind charge exchange in cometary atmospheres III. Results from the Rosetta mission to comet 67P/Churyumov-Gerasimenko. *Astronomy & Astrophysics*, 2019. doi: 10.1051/0004-6361/201834881.

Edward J. Smith, Bruce T. Tsurutani, James A. Slavin, Douglas E. Jones, George L. Siscoe, and D. Asoka Mendis. International cometary explorer encounter with Giacobini-Zinner: Magnetic field observations. *Science*, 232(4748):382–385, 1986. ISSN 0036-8075. doi: 10.1126/science.232.4748.382.

A Additional events

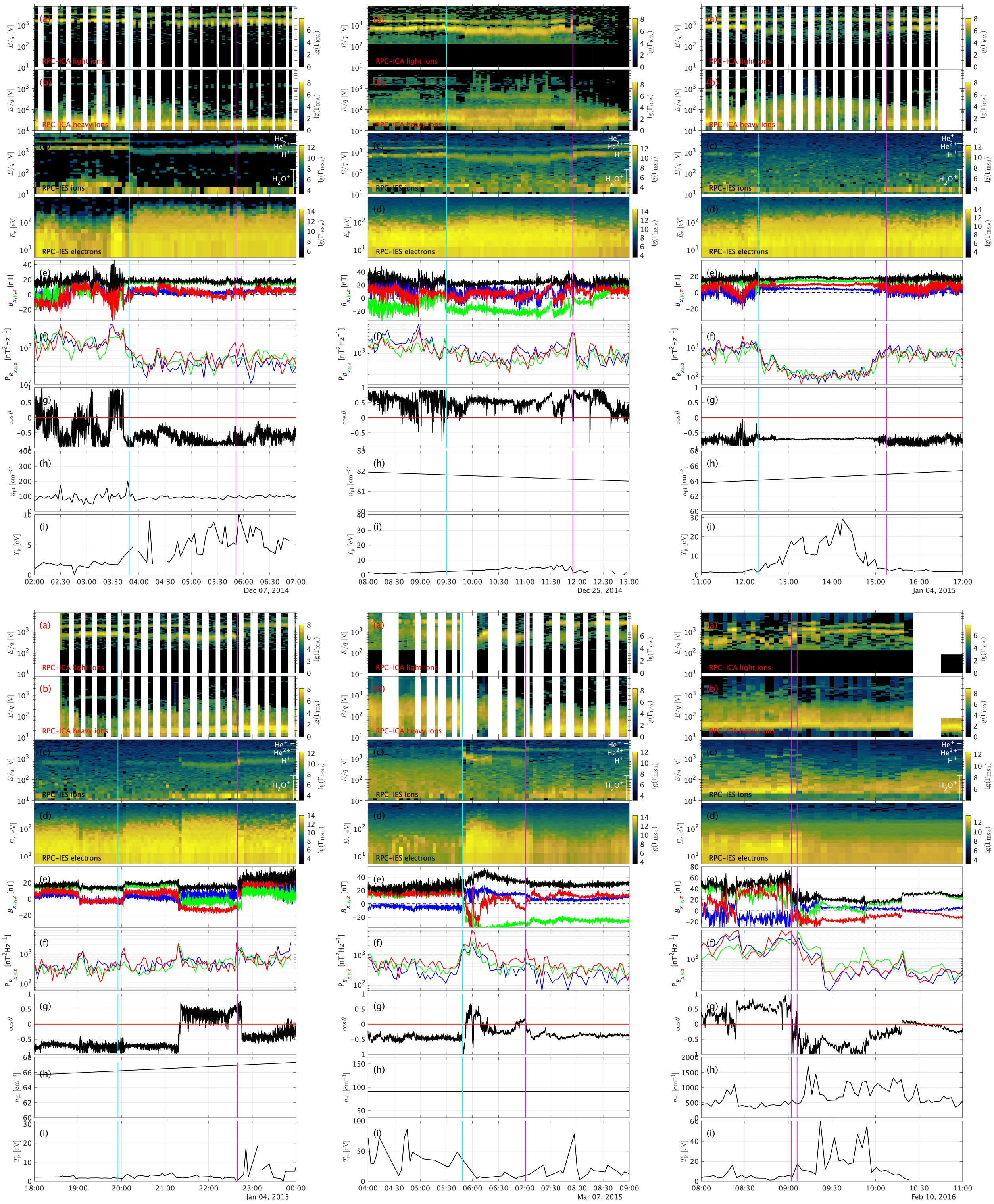

Figure 6: Observations of the plasma for the events shown in Table 1. Format is the same as in Figure 1.

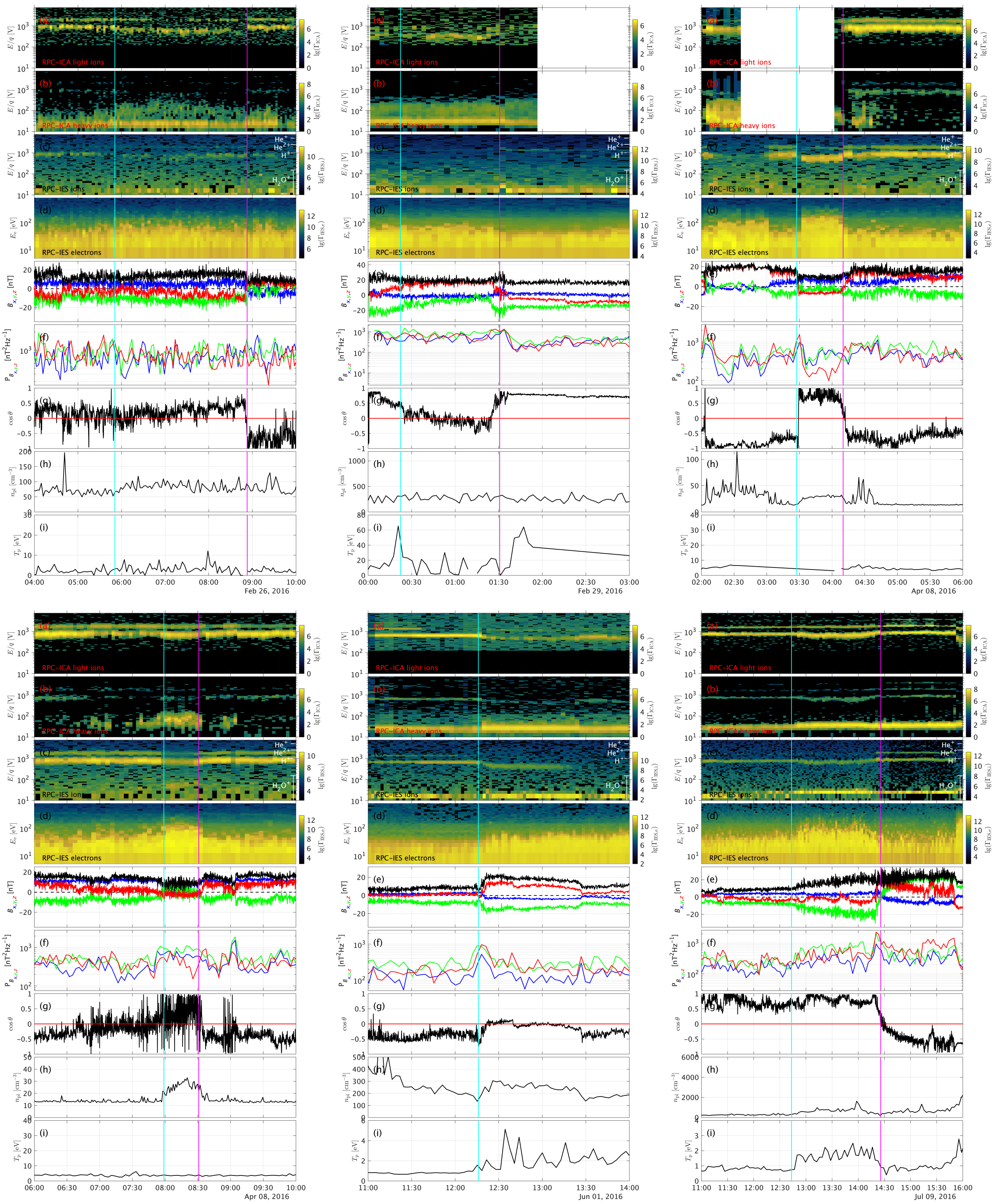

Figure 7: Observations of the plasma for the events shown in Table 1. Format is the same as in Figure 1.